Journal of Structural Geology, Vol. 9, No. 2, pp. 233 to 242, 1987
Printed in Great Britain

0191-8141/87 $03.00 + 0.00

Finite strain effects in experimental mullions

DIMITRIOS SOKOUTIS

The Hans Ramberg Tectonic Laboratory, Institute of Geology, Uppsala University, Box 555, S-75122 Uppsala, Sweden

(*Received* 7 *April* 1986; *accepted in revised form* 22 *August* 1986)

Abstract—Mullions are cylindrical structures developed at the interface between rocks of different competence shortened along the layering. Natural examples include phyllosilicate-rich meta-igneous sheets and massive sulfides in silicate country rocks. In axial profiles they consist of rounded lobes convex into the less competent material which alternate with sharp cusps pointing toward the more competent material. Mullions have been produced experimentally in incompetent single layers of silicone putty (viscosity $\eta_L = 2.9 \times 10^4$ Pa s and power law exponent $n = 1$) embedded in a strain-rate softening host of plastilina + silicone putty mixture ($\eta_h = 5.5 \times 10^6$ Pa s and $n = 7.1$). The initiation, development and changes in geometry of mullions in the two interfering interfaces of a single incompetent layer shortened along its length by pure shear, are reported. Up to ~10% bulk shortening (% BS) gentle flexures develop first in one interface, then, by ~17% BS, in both. These rounded irregularities become cuspate at ~25% BS. Where a lobe develops on one contact, a cusp is slightly preferred on the opposite side. Such antisymmetric mullions contrast with the symmetrical (pinch-and-swell) mullions predicted by Smith, but are like natural examples and those figured in the literature. The amplitudes of the cusps increase while their wavelength range decreases with finite shortening. It has been found that mature cusps distort but do not transgress the original contact even if the viscosity contrast is ≈1/1000. Beyond 40% BS, cusps either mature to flames or combine to horns, and after 60% BS even the last surviving mullions cease to amplify dynamically and the layer only thickens uniformly. Most stages seen in the models can be matched by natural field examples.

INTRODUCTION

MULLIONS are cylindrical deformation structures developed at the interface between rocks which have deformed with different competence (Figs. 1 and 2). In axial profiles (Fig. 3), mullions consist of rounded lobes convex into the least competent material alternating with sharp cusps pointing towards the more competent material (Fletcher 1982). Mullions frequently extend for long distances along their axes. They are known in deformed rocks of all ages and origins. They are found on a wide range of scales from a few mm to tens of km (Holmquist 1928, Ramsay 1967), although Park (1983, p. 26) has suggested that the term mullion be restricted to rodding structures which have dimensions of tens of cm.

Mullions and their implications have been described and debated since 1891 and at times confused with, among other phenomena, slickenside-grooving and rodded or constricted pebbles (see, e.g. Whitten 1969, p. 314, Wilson 1961, p. 510, Dennis 1972, p. 194).

Read & Phemister (1926) suggested that mullions result from the interaction of two deformations. He assumed that a phase of stretching parallel to the length of the mullions was superposed on an earlier phase of compression. Holmquist (1928) attributed mullions to a single deformation and to relative 'plasticity' (competence) of the two materials. Wilson (1953) considered that mullions could form in a single compression. Most modern workers would probably agree with Wilson, although prismatic hornblende crystals have been observed oriented parallel to the long axes of mullions suggesting possible longitudinal extension (Dennis 1972, p. 196). Four varieties of mullions were recognized and defined by Wilson (1953, 1961): fold mullions, bedding mullions, cleavage or foliation mullions and irregular mullions.

Only fold mullions generated in an incompetent layer shortened along the layering will be considered in this paper.

Ductility dependence

In nature it is common for the same layer to show mullions superposed on earlier folds, boudins or mullions. Such relationships indicate that many natural polyphase deformations involve changes in the ductility contrast between the layers at separable stages of deformation. Such changes in ductility contrast presumably occur in response to differences in strain rate, pressure, temperature, and any mineral transformations that take place during the strain (Ramsay 1982). Any change in the water content and grain size of say, an initially competent dyke would influence its mechanical properties rendering it incompetent compared to its surroundings (Fig. 1f) (Ramsay 1982, fig. 10). Mullions are typically developed in strongly deformed rocks of high metamorphic grade (e.g. Fig. 2c), with some exceptions in regions of relatively low-grade metamorphism (Wilson 1961, p. 511). Potash salts are also less competent than sodium salts and many of the difficulties of successfully predicting deformed structures in layers of deformed potash may relate to this fact (Talbot, personal communications 1983).

Another example of the potential economical importance of mullions is illustrated by Maiden *et al.* (1987), who suggests that most massive sulfide bodies have mullioned boundaries with economic concentrations of ore in the cusps and uneconomic widths in between.

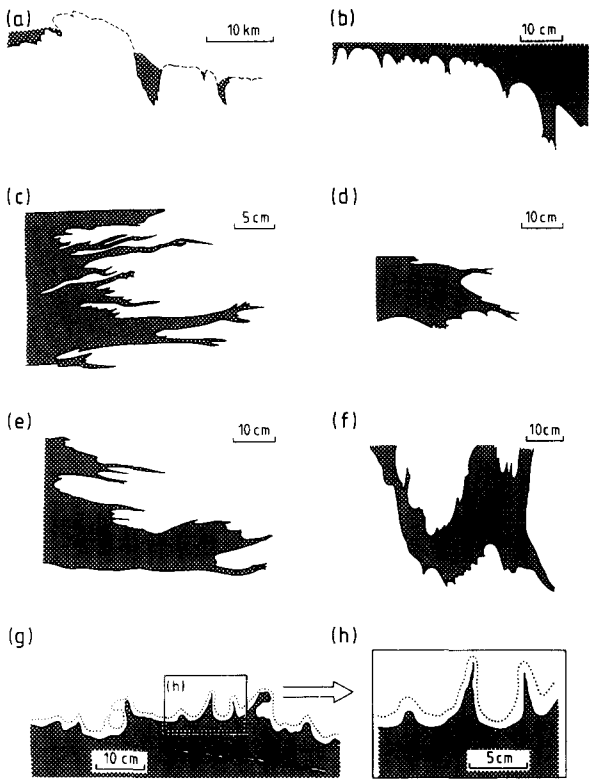

Fig. 1. (a) An example of extremely large mullions found in the French Alps between basement gneisses and Mesozoic sedimentary rocks (after Ramsay 1967, fig. 7-43). In this and all following figures the less competent materials are darkened. (b) Mullions in a dyke of hornblende schist in a granitic gneiss (after Ramsay 1967, fig. 7-45). (c) Advanced stage of growth of flame-like cusps of tholeitic dykes in biotite gneisses deformed together at granulite metamorphic facies in S. Africa (after Jackson & Zelt 1984, fig. 14c). (d) Part of metabasic dyke in the Sand River gneisses, the Causeway, Transvaal, S. Africa (traced from photo by C. J. Talbot). (e) Mature cusps along the contact of a mafic dyke, the Causeway, S. Africa. The dyke mainly consists of green-brown hornblende and plagioclase (after Fripp 1981, fig. 37). (f) Mullions on a folded basic dyke indicating that the dyke became incompetent in comparison with the surrounding gneisses. Lewisian complex, Scotland (after Ramsay 1982, fig. 10). (g) Cusps and flames in an argillaceous layer embedded in arenaceous beds on W shore of Eknö, Västervik area, Sweden (after Gavelin 1984, fig. 13). The folded competent pegmatite vein on the right demonstrates that the compression was along the layer. The dots indicate the trace of layering. (h) Magnified part of (g).

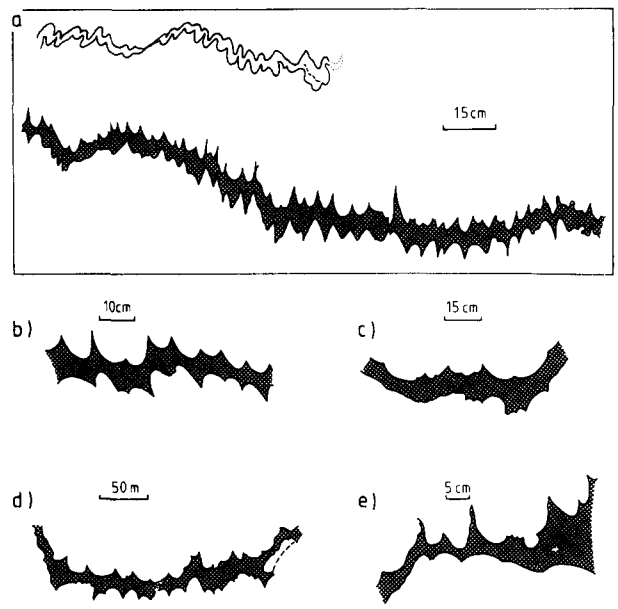

Fig. 2. Field examples illustrating the geometry of mullions for the two-interface case. (a–b) Mullions in gneisses of the Moine complex at Loch Monar, Scotland. Folds on the top left of (a) indicate that compression was along the layer (traced from photo by C. J. Talbot). (c) Early stage of development of mullions in an amphibolite sheet in a layered biotite gneiss host, S. Africa (after Jackson & Zelt 1984, fig. 14A). (d) Deformed porphyry dyke in gneiss (after Cobbold 1969a, fig. 14, map A). (e) Mullions in Moine gneiss, Loch Monar, Scotland (after Dennis, fig. 10-27).

Theory

Biot (1965) offered a qualitative explanation for the development of mullions and showed that the force F acting on the interface in the x-direction is

$$F = \dot{e}_x(\mu_A - \mu_B) \sin \alpha \qquad (1)$$

per unit arc length (Biot 1965, fig. 2A), where μ_A and μ_B are the viscosities in medium A and medium B, and α is the slope angle of the folded profile.

Dieterich & Onat (1969) shed some light on the formation of mullions when they introduced a numerical approach to the study of finite, quasistatic, plane deformations in single plane interfaces between viscous solids with initial sinusoidal disturbances. They concluded that mullions of the type they simulated are due to the growth of interfacial irregularities between two layers with different Newtonian viscosities. Biot (1965, fig. 2B) and

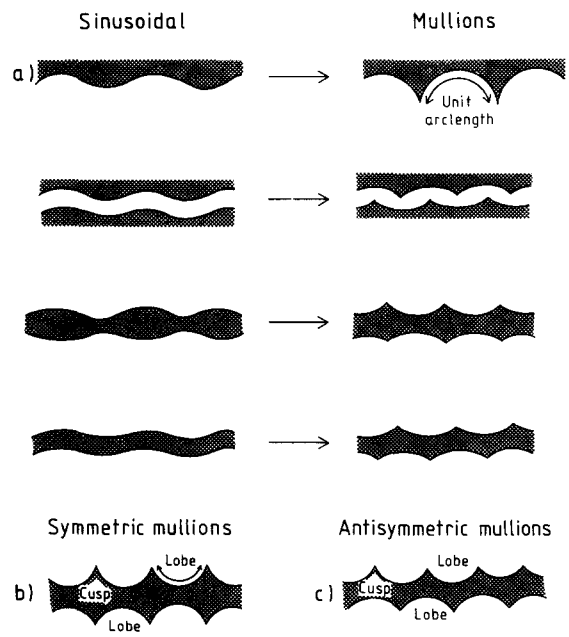

Fig. 3. (a) Figure illustrating the deviation of structures from an early sinusoidal shape (L.H.S.) to the development of mullions (R.H.S.) under pure shear conditions. (b) Symmetric mullions, cusp opposite to cusp, as predicted by Smith (1975, fig. 11). (c) Antisymmetric mullions, cusp opposite to lobe, as in the finite shortening experiments and most natural examples. (Cobbold (1975) used symmetric and antisymmetric in the opposite sense, but his terminology is not followed here.)

Ramberg (1970, fig. 2) illustrated how the velocities involved in buckling of the free surface of a compressed infinite half-space change the symmetry of an initial sinusoidal form towards a cusp and arc profile with progressive shortening. "The lack of constraint from a compressive stress normal to the surface at the flanks of the buckles allows the flanks to bulge out to make the anticlines wide and rounded and the synclines narrow and pointed for half-spaces whose surfaces face upward. For half-spaces with a downward facing surface the anticlines become narrow and pointed and the synclines wide and rounded. The normal velocity has a similar effect on the shape of the surface buckles as has the tangential velocity, accentuating the cusp and arc form of folds" (Ramberg 1981, pp. 155–156).

Smith (1975) introduced a linear hydrodynamic stability theory which attributes the onset of folding, boudinage, mullions, and inverse folds in single layers in infinite half-spaces to the same first order instability during plane strain shortening. The different geometries of each structure are due solely to differences in sign for particular factors in the same general equation. He concluded that the formation of mullions is due to compression along a layer which has a viscosity lower than that of the surrounding matrix. A dominant wavelength for the mullions depends on the thickness of the incompetent layer and the ratio of the viscosities of the layer (μ_L) and the host (μ_H). In 1977 Smith generalized his earlier linear stability theory to a form more applicable to deformed rocks by including non-Newtonian materials. The introduction of non-Newtonian rheology into the viscous problem alters the constitutive perturbation relation which becomes mechanically anisotropic in the sense that normal strain rates are lower than tangential strain rates at the same location. As a result the dominant wavelength of each category of instability is altered, and dynamic growth rates are increased (Smith 1977). The instabilities leading to folds, boudins, mullions, and inverse folds are progressively weaker so that, although folds are likely in viscous single layers, boudins and mullions are only likely if the host material(s) strain soften, and inverse folds are unlikely even in strain softening hosts. However, linear theory is constrained to infinitesimally small strains.. The mathematics become non-linear at finite strains and numerical or material modelling is currently necessary to explore how mullions develop with continued strain.

Experimental approach

An interesting difference between mullions in theory and fact is that Smith's (1975, 1977) and Fletcher's (1982) theories predict that all mullions should be symmetrical (or pinch-and-swell-like) (Fig. 2b), whereas the vast majority of natural examples seen by the author and his colleagues are antisymmetrical or fold-like (Fig. 2c). Cobbold (1975) alluded to this difference and used field evidence to suggest that the symmetry may change during finite strain.

Ramsay (1967) and Cobbold (1969) succeeded in generating mullions experimentally in a single interface between Newtonian fluids at high finite strain with high viscosity ratios. Cobbold (1969) went further and measured the growth rates of his experimental mullions.

However, in the absence of a length scale provided by having two interfaces on either side of a single layer, these had no preferred wavelength. I know of no experimental work on mullions in single layers other than that reported here. This work is an attempt to explore how an incompetent Newtonian layer embedded in a non-Newtonian host behaves when shortened along its length by pure shear. Particular emphasis is placed on the changes in geometry of the mullions during deformation.

METHOD

Material properties

Preliminary experimental investigations established that millions form spontaneously where the viscosity ratio m ($=\eta_{LAYER}/\eta_{HOST}$) is about 1/10, with power law exponents of the host in the range of 1.31, 1.41, 1.47, but only when bulk shortening reaches between 60 and 75%. It was found empirically that by increasing the viscosity ratio, mullions generate at much lower bulk shortening. Such a viscosity ratio can easily be achieved between a Newtonian single layer and non-Newtonian host material, especially if the power law exponent of the host is high. This is because, while the Newtonian material has a constant viscosity at all strain rates, the effective viscosity of the non-Newtonian host decreases with an increase in the applied strain rate.

Three materials were used: (1) a silicone bouncing putty 'Rhodorsil Gomme GSIR', supplied by Rhône-Poulenc of Paris, representing the incompetent layer in all experiments, (2) a homogeneous mixture of plastilina (50% red and 50% white) and Rhodorsil Gomme, of 67% to 33% mixture by weight, respectively, to represent the host, and (3) a mixture of plastilina (50% red and 50% white, as before) and Rhodorsil Gomme, 75% to 25% by weight, respectively, as an alternative host. Such mixtures were chosen because they have sufficient yield strengths in blocks of 12 × 12 × 8 cm to prevent collapse during model preparation.

Plastilina is a Swedish version of plasticine produced by Harbutts Plasticine Ltd., Bath, U.K. The exact chemical compositions of both plastilina and plasticine are trade secrets but are likely to be mixtures of polymers (oils and dyes) with carbonate fillers (McClay 1976). Red, black, and white plastilinas of Beckers Dekorima (Sweden) have been investigated by Weijermars (1986). The liquid phase in plastilinas is extremely small compared to that in, for example, Bouncing Putties. The heterogeneous filler contains quartz, kaolinite, hydrated halloysite, K-feldspar, and microcline. Red plastilina is coloured by a liquid of dissolved pigments, and white plastilina is coloured by barytes, and includes wurtzite and periclase, in addition to the minerals listed above.

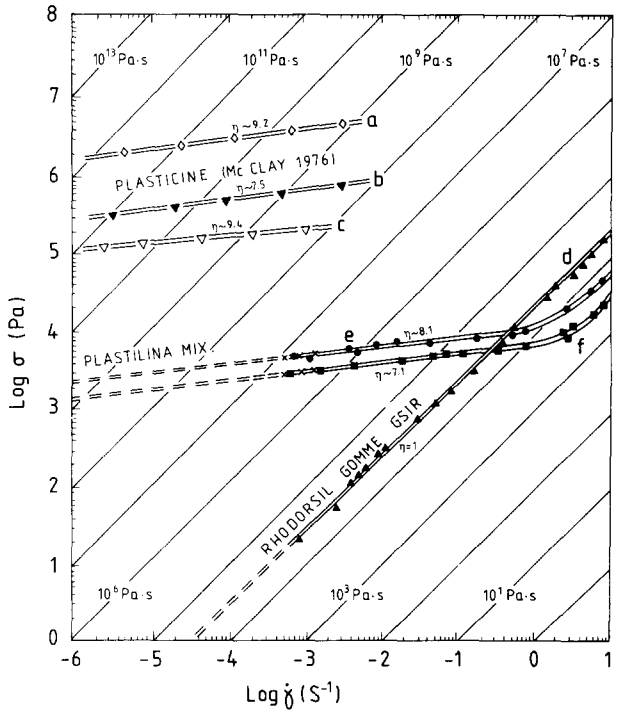

Fig. 4. Flow curves (a–f) of plastilina-like materials where $\dot{\gamma}$ represents the engineering strain rate ($\dot{\gamma} = 2\dot{\varepsilon}$, $\dot{\varepsilon}$ = natural strain rate). Materials a–c: Standard hard, standard white and specially soft plasticine, respectively, of Harbutts Plasticine Ltd. (Britain) at 25°C (from McClay 1976, fig. 2). Material d: Bouncing Putty (Rhodorsil Gomme GSIR) of the Société des Usines Chemiques Rhône-Poulenc (France). Material e: Mixture of red and white plastilina (50% of each) and Rhodorsil Gomme of the weight percentage ratio 75 : 25, respectively. Material f: Mixture of 67 weight % of equal parts red and white plastilina with 33 weight % Rhodorsil Gomme. Materials (d–f) were at steady state flow, measured by both rotor-viscometer and HAAKE extrusion viscometer at 24°C.

Flow curves were determined using a HAAKE steady state extrusion viscometer. These curves were closely matched by other curves for the same material using a cylindrical viscometer constructed by R. Häll (Weijermars 1986).

The silicone Bouncing Putty used for the single layers in all experiments is Newtonian at all the investigated strain rates. However, the addition of plastilina changed the behaviour of the host to non-Newtonian with a power law relationship, $\dot{\varepsilon} = c\sigma^n$, where the coefficient c is a constant and n is the power law exponent. The n-value is equal to the inverse of the slope on the graph (Fig. 4) of strain rate (s^{-1}) against stress (in Pa).

The 67% to 33% plastilina–silicone putty mixture had a power law exponent $n = 7.1$. The plastilina–silicone putty mixture of 75% to 25% had a power law exponent $n = 8.1$. Since the power law exponents are greater than 1 the mixtures strain-rate soften.

At the range of strain rates used in the experiments described here (4.5×10^{-4} s^{-1} to 1.36×10^{-3} s^{-1}, Fig. 5b), the viscosity of the single layer of Rhodorsil Gomme was 2.9×10^4 Pa s. The effective viscosity of the 67% to 33% plastilina–silicone putty mixture ranged between 5.5×10^6 and 2.2×10^6 Pa s. This means that the bulk m ranged from 1/190 at the beginning (~8% bulk shortening) to $m = 1/76$ at the end of the experiments in which this mixture was used (~75% BS). The effective viscosity of the 75% to 25% plastilina–silicone putty mixture ranged between 9.3×10^6 to 3.67×10^6 Pa s. This implies a range of m during the experiments of $m = 1/321$ at the beginning (~8% BS) to $m = 1/127$ at the end (~75% BS). The bulk viscosity ratios in all experiments therefore, neglecting possible local changes in m with respect to local changes in the shape of the layer, changed by a factor of less than 2 (Fig. 4). Although most of the models were deformed up to 75% BS, in order to study geometric changes in the shape of the mullions, measurements of growth rates concentrated on experiments with bulk shortening of less than 50%.

All viscosity measurements and model deformations were made at a temperature of 24 ± 2°C.

Model construction

Single plane layers of constant thickness were embedded in a more competent host. The mixtures of plastilina and silicone putty were used to represent the competent host, while the incompetent plane single layer was represented by 'Rhodorsil Gomme GSIR' silicone putty.

For each experiment a rectangular parallelepiped (12 × 12 × 8 cm) of the host plastilina–silicone putty mixture was prepared (Fig. 6). This was then cut precisely into two equal halves. The planar incompetent single layer was placed in between, and the three components pushed together using perspex plates.

Models of two types were constructed. One group had a 3-dimensional rectilinear grid of very thin (≈0.01 mm) layers of carbon powder inserted in the host matrix within ≈0.4 cm of the embedded layer. Smith (1979) suggested that cusps penetrate the component host and the carbon marker layers were included to test this possibility. The carbon markers were intended to be passive but were abandoned after they were suspected of exerting some influence on the wavelength of the mullions. Smith (1979) has pointed out that a straight passive marker line at some y position (where $y = 0$ is the interface) will become deformed into a wavy pattern. In a strongly non-Newtonian host the most rapid deformation would be expected to occur in marker lines located a distance $y = \lambda/4$ away from the interface (Smith 1979). The carbon markers in the models described here were at $y = \lambda/\geqq 4$.

A second group of experiments had no such markers in the host. These had two functions: (1) to check the suspicion that the carbon markers had influenced the dominant arc length, and (2) to find at what thickness an incompetent layer reacts as two independent interfaces rather than as a single layer, when the strains at each interface influence one another.

Model deformation

The embedded incompetent layers in the more competent host were shortened along their length in a pure

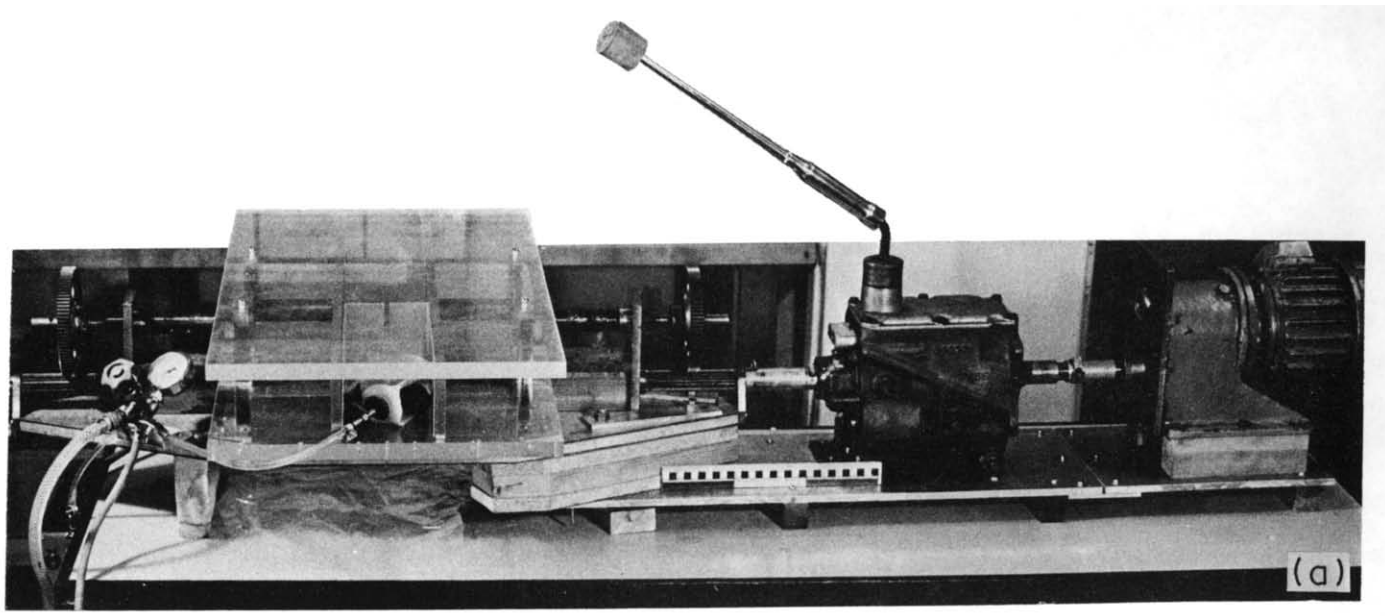

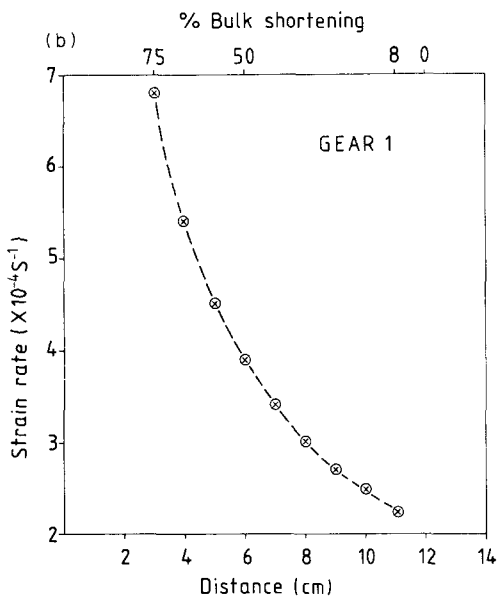

Fig. 5. (a) The pure shear box at the Hans Ramberg Tectonic Laboratory at Uppsala, Sweden. Rule is cm scaled. See Appendix for description. (b) Figure showing the change in natural strain rates ($\dot{\varepsilon}$) of the pure shear box with progressive bulk shortening using gear 1.

shear box described in Appendix 1 (Fig. 5a). The outer surfaces of the whole block were lubricated with light machine oil and then deformed by pure shear in the pure shear box. Compressive force was applied so that the incompetent single layer was shortened precisely parallel to its boundaries. The deformed model was removed and sectioned parallel to the *xz*-plane (Fig. 6) at different stages of conventional bulk shortening (calculated as $(L_U - L_D/L_U \cdot 100$ = percentage bulk shortening, % BS, where L_u is the undeformed length and L_D the length after deformation). This allowed study of the initiation and development of spontaneous mullions, as well as any changes in their geometry as the strain progressed.

RESULTS

The formation and development of mullions were studied in layers ranging in thickness from 0.1 to 0.5 cm

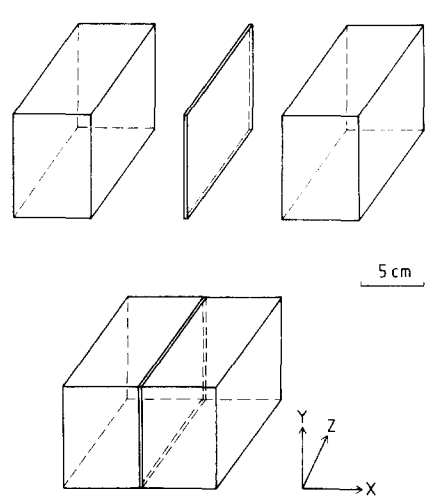

Fig. 6. The model parts before and after assembly. Direction of compression along the *xy*-plane, direction of extension along the *yz*-plane. Rigid perspex plates on top and bottom of the pure shear box prevent any movement along the *xy*-plane.

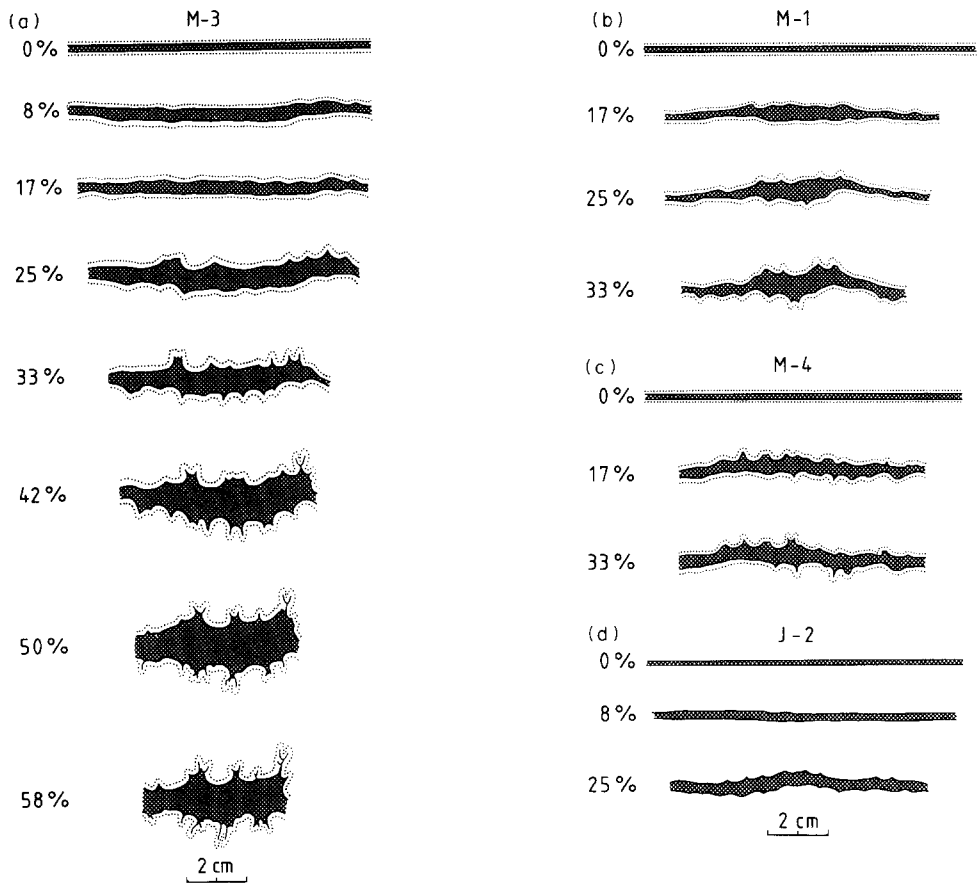

Fig. 7. Experimental mullions at different stages of bulk shortening. (a) Model M-3: Layer consists of material d, host of material f. Dots indicate carbon marker. (b) Model M-1: Layer material d, host material e. (c) Model M-4: The same materials as in M-3. (d) Model J-2: Model materials as in M-3. No carbon markers. For model materials, see Fig. 4.

under identical loading conditions with a constant starting viscosity contrast of $m = 1/190$ or $m = 1/321$.

When the thickness of the incompetent layer exceeded ~0.4 cm, the two interfaces deformed independently. Mullions developed in all cases independent of thickness, with the only difference that above ~0.4 cm there is no correspondence between spontaneous structures in the opposite sides of the layer. Figures 7(a) & (b) illustrate the development of mullions at different stages of bulk shortening.

There was no sign of any separation of the incompetent layer from the matrix at any stage of any of these experiments.

The development of mullions

The general pattern of mullion development was the same in every experiment.

(1) Up to ~10% bulk shortening (BS) the incompetent single layer thickened uniformly and gentle rounded flexures developed in one or other of the two interfaces.

(2) The interface with the largest deflection amplitude affected the opposite side of the incompetent layer so that by ~17% BS gentle rounded irregularities developed in both interfaces.

(3) Definite cusps pointing into the competent host were obvious at ~25% BS. Both interfaces had the same number of cusps and lobes (with 1 or 2 cusps difference), but some of these were better developed than others. Systematic measurements indicate that where a lobe developed at one interface of the incompetent layer, a cusp was slightly more likely to develop on the opposite side (Fig. 8). Such antisymmetric or fold-like mullions were in direct contrast to the theoretical predictions based on linear stability analysis (Smith 1977) but in agreement with most field observations.

(4) As the bulk shortening increased to ~33% the wavelength of the cusps decreased while their amplitudes increased. Soon after this stage a casual inspection might suggest that the cusps penetrate the competent matrix. At this stage, those cusps which started from irregularities of largest (but still microscopic) initial amplitude tighten and they close, to form structures which will here be called flames (Fig. 9). A flame is that part of a cusp of the incompetent material which has closed to negligible thickness. In the experiments reported here, cusps tightened to flames at ~33% BS.

(5) At ~50% BS and beyond, one of two possibilities occurred: cusps either matured to flames, or the cusps combined to horns, when two cusps combined and the small intervening lobe moved away from the incompetent layer (Fig. 9).

(6) Horns subsequently closed to compound horns at ~50% BS, branched flames at ~54% BS, and dendritic flames at ~58% BS (Fig. 9).

(7) Beyond 60% BS even the last surviving mullions

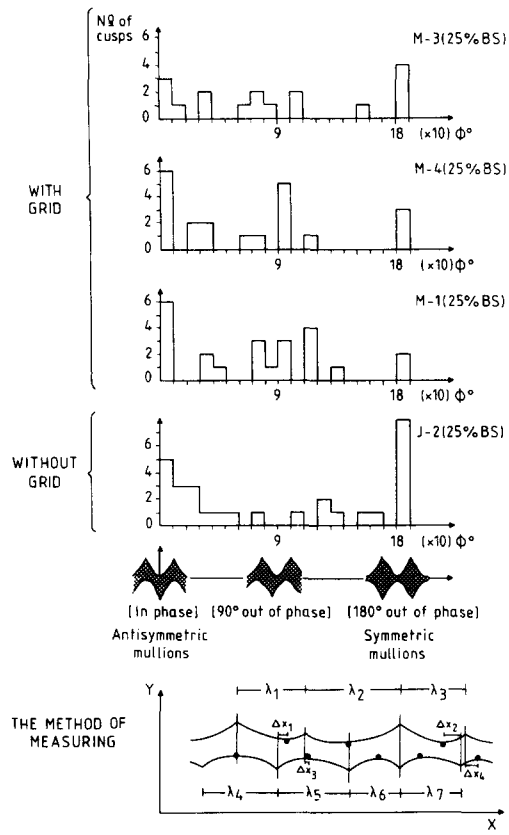

Fig. 8. Suggested nomenclature for mullions in two interfaces according to phase shift (ϕ). Measurements used to plot the histograms, for finding the most preferred geometrical shape of the experimental mullions. The histograms are valid up to ≈25% bulk shortening when the two interfaces still influence each other. In these measurements, ϕ is the angle of shift ($\phi = \Delta x_i/\lambda_j \cdot 360°$, where i and j are positive numbers, λ is the wavelength, Δ_x is the horizontal displacement of a lobe with respect to the cusp on the opposite side). Dots indicate the 'maximum amplitude' of the lobes towards the incompetent layer.

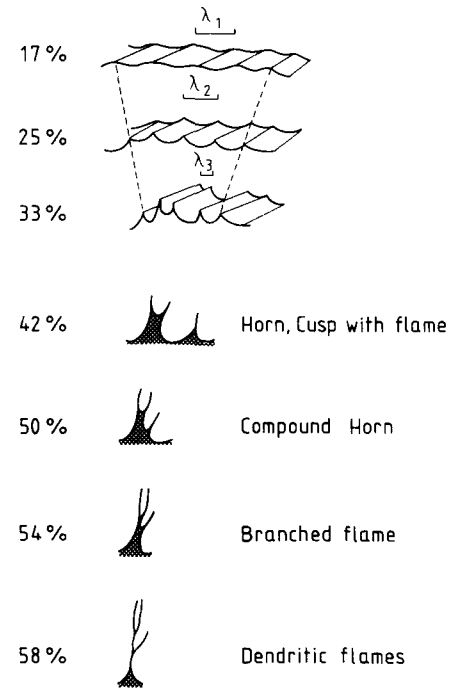

Fig. 9. Decrease in wavelength, increase in amplitude and the development of flames, horns, compound horns, branched and dendritic flames. Only one of the two interfering interfaces is shown (from Experiment M-3).

ceased to amplify although the layer still thickened uniformly.

Various combinations of flames, horns, compound horns, or even branched and dendritic flames are by no means unusual in the same shortened single layer, either in the models, or in the field (Figs. 1c & e and 10). Some of the models deformed with carbon markers gave the impression that dominant wavelengths were involved (as predicted by infinitesimal strain theory, Smith 1977) but models without carbon markers showed no such tendency. This suggests, but does not prove, that mullions at finite deformation may not have a dominant wavelength.

Growth rates

Although growth rates cannot be determined for natural structures, the study of growth rates in laboratory experiments (by measurement of their amplitude) allows a useful check on theoretical models of how such structures evolve. Smith's theory (1977, p. 318, fig. 8) predicts growth rates for mullions for infinitesimally small strains in strain-rate softening materials ($n > 1$) but such predictions are usually assumed to be still relevant at small finite strains (Neurath & Smith 1982, p. 225). The early stages of bulk shortening may therefore be used to compare experimental results with theoretical predictions. The normalized growth rates γ, of initial disturbances (i.e. growth rate γ = normalized amplitude divided by natural strain, BS, parallel to the layer) are theoretically independent as long as their amplitudes are small (Smith 1977, Neurath & Smith 1982). The growth rates of mullions when $m \ll 1$ are expected to be strongly dependent on both m- and n-values (Smith 1977). The normalized growth rate, γ, for experiments M-1 and M-3, is plotted against overall strain in Fig. 11(b). The slope of the curve at any point on such graphs equals the growth rate at that point (Fig. 11b). The growth rate can be seen to increase in the initial stages but to level off after a characteristic amplitude has been reached. Thereafter the amplitude of the cusps actually decreases because they close to flames and most of the incompetent material is squeezed back into the incompetent layer. The flames continue to increase in amplitude, despite apparently being closed, but eventually even they cease to grow at ≈60% BS.

DISCUSSION

It has been suggested that because the stresses are higher in the competent host, the host material plays a more active rôle in the deformation of an incompetent single layer. Thus Talbot (1982) pointed out that strains in incompetent single layers are induced by strains of the surrounding more competent country rocks. Fletcher (1982, p. 52) went further and argued that "the strength

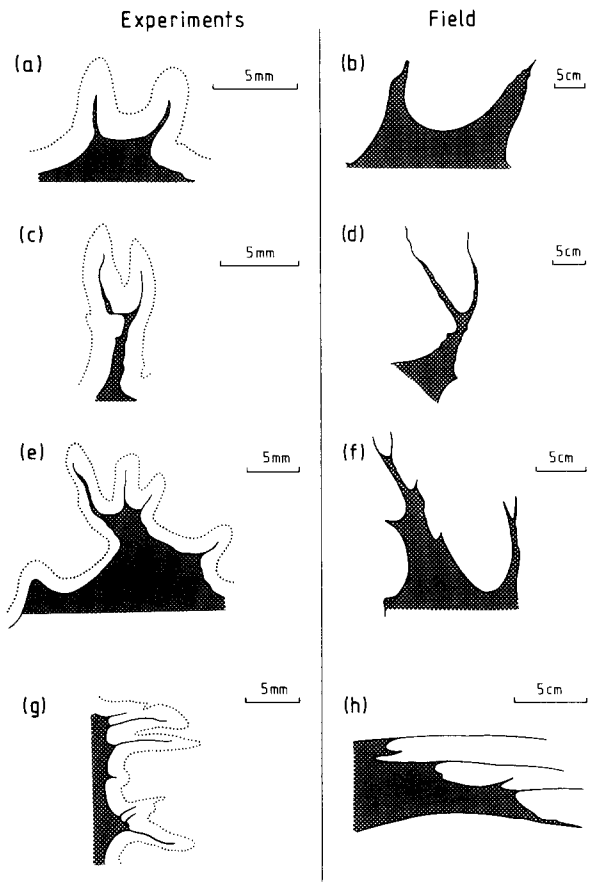

Fig. 10. Comparison of details between mullions in Experiments M-3 and J-2 (left column) and natural examples (right column). Notice the absence of transgression of the carbon markers by the cusps. (b) Competent host, quartzite, incompetent mica schist. Nufenenpass, Central Switzerland (after Ramsay 1982, fig. 7). (d) Competent host, augen gneiss, incompetent amphibolite. Nolsterbysundet, NE Uppland, Sweden (traced from a photo by the author). (f) Competent host, gneiss, incompetent, mainly green-brown hornblende and plagioclase. Causeway, S. Africa (after Fripp 1981, fig. 36). (h) Competent host, red gneiss, incompetent amphibolite. Malmplatsen, NE Uppland, Sweden (traced from photo by the author).

of the instability is proportional to the power law exponent of the more competent medium".

The experiments reported here have indicated that before propagating to both interfaces, the initial process starts in one (presumably that with the greater microscopic irregularities). The gentle flexures which develop in one interface influence the opposite interface and cusps form from the resulting initially gentle flexures before maturing to flames, horns, compound horns, branched and dendritic flames.

There is no obvious reason for not accepting Smith's (1977) mathematical model for the mullion (or 'inverse boudinage', Smith 1975) instability. As predicted by Smith (1975, 1977) and Fletcher (1982), pinch-and-swell instabilities (symmetric mullions) initiated and amplified in all models described here, particularly in the absence of a grid of carbon powder (Fig. 8). What the infinitesimal theory does not predict or explain is the subsequent fold-like geometry of all the experimental incompetent layers at significant bulk shortening (~25% BS).

The fold-like geometry

The histograms plotted in Fig. 8 suggest that the early fold-like geometry was favoured by the carbon powder layers nearby. The tendency to fold-like geometry was reduced, but not at all removed, in the models without carbon layers. The initial pinches-and-swells increased in number when no carbon markers were present. The histograms in Fig. 8 are only valid up to ≈25% BS, when the two interfaces still influence each other; at higher bulk shortening we are in effect dealing with two independent interfaces. Measurements on the experiments reported here at BS < 25% do not resolve whether pinch-and-swell-like geometry precede the fold-like geometry.

Competence contrast

Ramsay (1982) suggested that mullions or 'cuspate-lobate shaped folds' indicate competence contrast of less than about 10. However, experiments reported here indicate that similar geometrical shapes can be formed at a great range of viscosity ratios, from m = 1/10 to ~m = 1/1000. Preliminary exploratory experiments with Newtonian single layers embedded in non-Newtonian hosts with n-values in the range of 1.37, 1.41 and 1.47 at competence contrasts of about 1/10 only resulted in mullions where bulk shortening exceeded 60%.

Intrusion (?)

The word intrusion or penetration is commonly used in discussions of cusp development (e.g. Smith 1979). Smith described the process as follows: "with interface-parallel shortening the tongues of the incompetent material will sharpen and penetrate more deeply . . . ." The carbon markers (e.g. Fig. 7a) demonstrate that intrusion (in the sense of transgression of the original contact by the cusp) does not take place, even when m = 1/321 and BS = 75%. The competent matrix squeezes the sides of a cusp or horn, creating a flame or a flame with branches and the soft material moves back into the main body of the incompetent layer. The lack of penetration illustrated by the experiments is strengthened by field evidence with appropriate markers (e.g. Figs. 1g & h).

The possibility of intrusion cannot be excluded at very high viscosity contrast (m > 1000), very fast strain rates, or if the host fails as a brittle solid.

Growth rates

The growth rates of cusps are similar at the two different viscosity contrasts tested (Fig. 11). Growth increases linearly until 20% BS but faster than predicted by Smith's infinitesimal theory (see also Cobbold 1969 and Dietrich & Onat 1969). Beyond 25% BS, the growth rate suddenly diminishes and beyond 35% BS reduces if only cusps are present. However, the growth rate of 'cusps and flames' becomes constant above 35% BS.

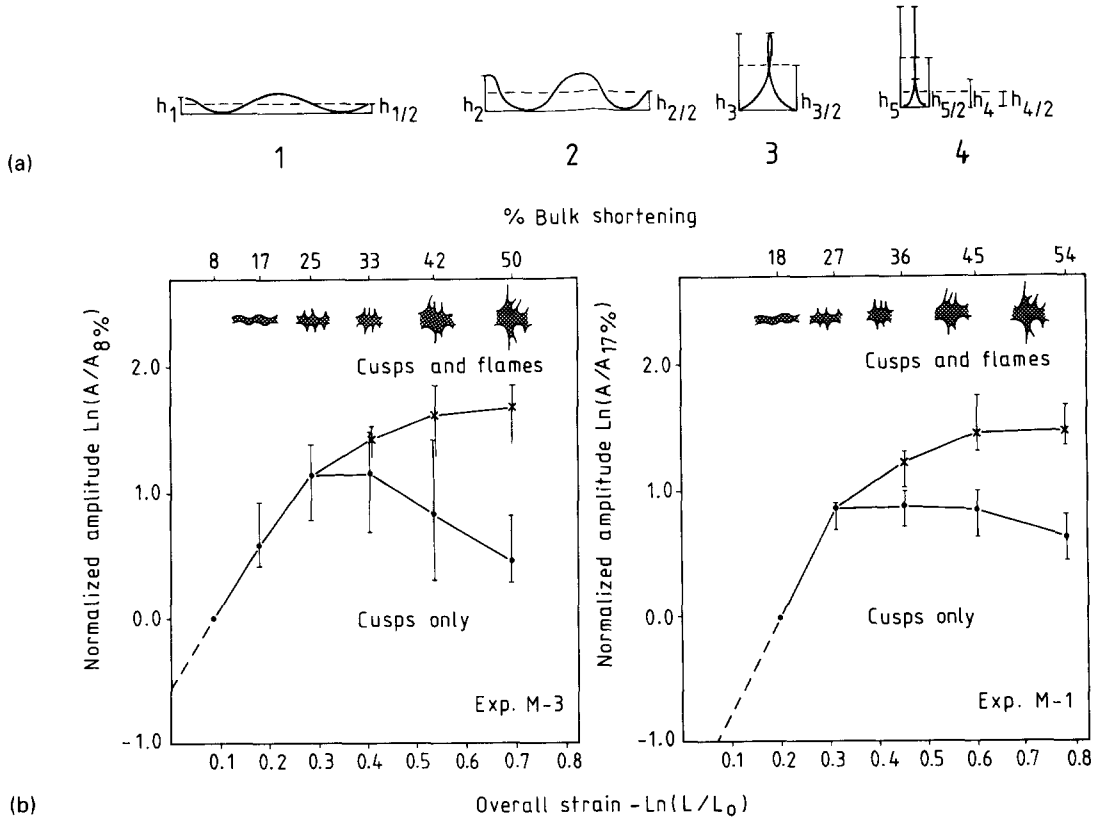

Fig. 11. Amplitude A of cusps with increasing bulk shortening. (a) Method of measuring. In cases like step 4 the amplitude of cusp and flame is $A_5 = h_5/2$ and that of the cusp is $A_4 = h_4/2$. (b) Amplitude of cusps plotted against overall strain. Results from Exp. M-1 (starting m = 1/321) and Exp. M-3 (starting m = 1/190). Each data point is the average of five individual cusps. The early growth rate [i.e. $\gamma = (\ln A/A_0)/(\ln L/L_0)$] does not continue to increase, but levels off and for the cusps only case, actually decreases. No measurements have been made on horns with flames or branched and dendritic flames.

The abrupt change in the early linear growth rate (below 25% BS on Fig. 11) approximately coincides with the transition from what Smith refers to as dynamic (structure forming) growth to kinematic (uniform thickening) growth. In other words, mullions grow at linear growth rates when the structures in the two interfaces interfere (or reinforce) each other—but display decaying growth rates and closure when the structures in the two interfaces no longer influence each other. Further work on the implications of this finding are in progress.

Practical problems restrict measurements of growth rates to ~50% BS. Unfortunately, no direct comparison can be made with Smith's (1977) theoretical growth rates for mullions since the experimental results belong to the finite stage. One explanation of the greater than predicted growth rate could be an overexponential growth of the disturbance as a consequence of the finite amplitude of the initial disturbance (as observed by Woidt (1978) in some theoretical models of Rayleigh–Taylor instabilities).

The decrease in growth rate of the cusps beyond 25% BS may be the result of strain-rate softening in the host. This reduces the viscosity contrast during shortening. Alternatively, different stress–strain conditions could develop because of the changing geometry of the interface. A third possibility is that there is no longer any co-ordination of the strains on the two contacts of the incompetent layer. As this stage is reached, every cusp or horn can be considered to develop individually in response to local stress–strain conditions. Figure 11(b) indicates that the cusps close as the shortening increases to ~50% BS. The flames cease to amplify, not only because of strain-softening of the host, but also because they are cut off from their supply of material from the incompetent layer; indeed, they lose material back to the incompetent layer and can be said to have retracted.

CONCLUSIONS

(1) Linear hydrodynamic stability does not explain the antisymmetric geometry of mullions which at finite strains seems to be preferred in experiments and in field examples. This preference for a fold-like symmetry appears to be a finite strain effect, as suggested by Cobbold (1975). The experiments reported here did not resolve whether the finite fold-like mullions initiated with a pinch-and-swell geometry.

(2) Even with m as high as ≃1/1000, mullions do not transgress their original contact, but actually close off and retract with increasing shortening.

(3) With starting viscosities of m = 1/321 and m = 1/190, the successive appearance of horns, flames, compound horns, branched and dendritic flames are indicators of significant shortening along the layer (≃40% BS).

(4) Measured growth rates of experimental mullions are larger than those predicted by Smith's (1977) infinitesimal theory, but this is a finite strain effect.

(5) Further investigations, both mathematical and experimental, are necessary to expand our knowledge of mullions, which are quite common in rocks deformed at high metamorphic grade, but which also occur in lower-grade rocks.

Acknowledgements—I would like to thank Professors C. J. Talbot and H. Ramberg for useful discussions and encouragement of this work. Dr H. Schmeling and R. Weijermars are acknowledged for comments and advice on material properties, respectively. Dr P. Cobbold kindly provided two of his unpublished B.Sc. theses. The manuscript has been improved by the comments of Professor J. Dennis and Dr P. Cobbold. Miss K. Gløersen is sincerely thanked for typing the manuscript and Mrs C. Wernström for drafting the figures.

REFERENCES

Biot, M. E. 1965. Theory of viscous buckling and gravity instability of multilayers with large deformations. *Bull. geol. Soc. Am.* **76**, 371–378.

Cobbold, P. R. 1969a. An experimental study of the formation of lobe and cusp structures by shortening of an initially sinusoidal contact between two materials of different viscosity. Unpublished B.Sc. thesis, University of London.

Cobbold, P. R. 1969b. Structural geology of the Val Camadra-Greina area, Ticino, Switzerland. Unpublished B.Sc. thesis, University of London.

Cobbold, P. R. 1975. Unified theory on the onset of folding, boudinage, and mullion structure: Discussion. *Bull. geol. Soc. Am.* **87**, 1663.

Dennis, J. G. 1972. *Structural Geology*. Ronald Press, New York.

Dieterich, J. H. & Onat, E. T. 1969. Slow finite deformations of viscous solids. *J. geophys. Res.* **74**, 2081–2088.

Fletcher, R. C. 1982. Analysis on the flow in layered fluids at small, but finite, amplitude with application to mullion structures. *Tectonophysics* **81**, 51–66.

Fripp, R. E. P. 1981. The Precambrian geology of the area around the Sand River near Messina, Northern Transvaal. Unpublished Ph.D. thesis, University of the Witwatersrand.

Holmquist, P. J. 1928. The relative plasticity of rock-masses under the influence of dynamic deformation. *Fennia* **50**, 1–13.

Jackson, M. P. A. & Zelt, G. A. D. 1984. Proterozoic crustal reworking and superposed deformation of metabasite dykes, layered intrusions, and lavas in Namaqualand, South Africa. International Union of Geological Sciences, Commission on Tectonics, Subcommission on Precambrian Structural Type Regions, Final Report (edited by Kröner, A. and Greiling, R.), E. Schweizerbart'sche Verlagsbuchhandlung, Stuttgart 1984, pp. 381–400.

Maiden, K. J., Chimimba, L. R. & Smalley, T. J. in press. Cuspate ore-wall rock interfaces, piercement structures, and the localization of some sulfide ores in deformed sulfide deposit. *Econ. Geol.*

McClay, K. R. 1976. The rheology of Plasticine. *Tectonophysics* **33**, T7–T15.

Neurath, G. & Smith, R. B. 1982. The effect of material properties on growth rates of folding and boudinage: experiments with wax models. *J. Struct. Geol.* **4**, 215–229.

Park, R. G. 1983. *Foundations of Structural Geology*. Blackie, Glasgow.

Ramberg, H. 1970. Folding of laterally compressed multilayers in the field of gravity. II. Numerical examples. *Phys. Earth Planet. Interiors* **4**, 83–120.

Ramberg, H. 1981. *Gravity, Deformation and the Earth's Crust*. Academic Press, London.

Ramsay, J. G. 1967. *Folding and Fracturing of Rocks*. McGraw-Hill, New York.

Ramsay, J. G. 1982. Rock ductility and its influence on the development of tectonic structures in mountain Belts. In: *Mountain Building Processes* (edited by Hsü, K. J.). Academic Press, London.

Read, H. H. & Phemister, J. 1926. The geology of Strath Oykell and Lower Loch Shin. *Mem. geol. Surv. Scotland*, sheet 102.

Smith, R. B. 1975. Unified theory of the onset of folding, boudinage, and mullion structure. *Bull. geol. Soc. Am.* **86**, 1601–1609.

Smith, R. B. 1977. Formation of folds, boudinage, and mullions in non-Newtonian materials. *Bull. geol. Soc. Am.* **88**, 312–320.

Smith, R. B. 1979. The folding of a strongly non-Newtonian layer. *Am. J. Sci.* **279**, 272–287.

Talbot, C. J. 1982. Obliquely foliated dikes as deformed incompetent single layers. *Bull. geol. Soc. Am.* **93**, 450–460.

Weijermars, R. 1986. Flow behaviour and physical chemistry of Bouncing Putties and related polymers in view of tectonic laboratory applications. *Tectonophysics* **124**, 325–358.

Whitten, E. H. T. 1969. *Structural Geology of Folded Rocks*. Rand McNally, Chicago.

Wilson, G. 1953. Mullion and rodding structures in the Moine Series of Scotland. *Proc. Geol. Ass.* **64**, 118.

Wilson, G. 1961. The tectonic significance of small-scale structures, and their importance to the geologist in the field. *Annls Soc. géol. Belg.* **84**, 510–517.

Woidt, W. D. 1978. Finite element calculations applied to salt dome analysis. *Tectonophysics* **50**, 369–386.

APPENDIX

Experimental equipment

The 'pure shear box' in the Hans Ramberg Tectonic Laboratory at Uppsala University (Sweden) is as follows.

(1) Two brass platens (70 × 2 × 8 cm) can be driven towards or away from each other by an electric motor through an intervening system of threaded rods at controlled rates, using a gear box. The maximum distance possible between the plates is 25 cm.

(2) The top and bottom of the volume where the deformation takes place are closed by 2 cm thick rigid perspex plates. This enables qualitative monitoring of the deformation of the top (and bottom) of a model during an experiment. However, all the various lubricants used to date tend to smear during an experiment and sectional studies are necessary for detailed measurements and photographs at different stages of the experiments.

(3) Telescoping L-shaped sidewalls supported by air bags sharing the same compressed air supply are used to confine the free ends of the model to a rectangular shape. The air pressure in the bags ($\simeq$0.15 kg cm^{-2}) is shown on a manometer and is released at appropriate intervals throughout an experiment. When the bulk shortening exceeds 50%, the initial L-shaped sidewalls can be replaced by others without disturbing the model.

(4) The top and bottom of the models reported here were lubricated with low viscosity motor oil to reduce shear along them.

The velocities of the moving plates were calculated for all four gears with and without model material inside and converted to conventional strains and strain rates. The velocity of the plates was found not to be influenced by the presence of any model. Gear 1 was used in all experiments because it gives the smallest variation in strain rates (Fig. 5).